Thrombocytopenia is one of the major problems encountered when treating esophageal varix or hepatocellular carcinoma (HCC), both of which are frequently observed in patients with advanced CLD. Thrombocytopenia also often hampers the treatment of hepatitis C virus (HCV)-related CLD (CLD-C) by interferon [1]. Thus, it is important to clarify the mechanism and establish the therapeutic strategy of thrombocytopenia in CLD. Because cirrhotic liver with advanced tissue fibrogenesis gives rise to portal hypertension, inducing splenic enlargement and congestion [2–5], splenomegaly has been considered to cause thrombocytopenia by increased sequestration and enhanced destruction of platelets [6, 7]. However, the exact pathogenesis of thrombocytopenia in CLD is not yet fully understood [8–11].

Of interest is the fact that the prevalence of thrombocytopenia is higher among patients with HCV-related HCC than in those with hepatitis B virus (HBV)-related HCC [12]. Such evidence suggests that HBV-related HCC may tend to arise in the liver with less advanced chronic injury than in that of patients with HCV-related HCC; it also raises the possibility that thrombocytopenia may be more severe in CLD-C than HBV-related CLD (CLD-B). To examine the latter possibility, it is necessary to compare the platelet count between the two groups with an adjustment for the degree of liver fibrosis or splenomegaly. However, previous studies in this area may have been hindered by the invasiveness of measuring portal blood pressure or liver fibrosis. More recent studies, however, have focused on the non-invasive prediction of liver fibrosis [13–16], taking into account the various limitations of liver biopsy [17–20]. In particular, recent evidence on transient elastography reveals that the liver stiffness values acquired by the elastometer correlate well to the fibrosis stages as determined by liver biopsies [21–24]. Similar optimal cut-off values of liver stiffness have also been reported for the diagnosis of cirrhosis in patients with chronic hepatitis B and C [25, 26].

In the study reported here, we sought to investigate whether the degree of thrombocytopenia in CLD differs according to virological etiology, namely, HBV or HCV. Since most of the patients enrolled in our study were outpatients, we measured liver stiffness in each patient instead of performing liver biopsy to assess the degree of liver fibrosis, which may raise an ethical concern. In addition to the non-invasiveness of the measurement, liver stiffness values may have the merit of being a continuous variate, which has a wider application to statistical analyses than a discrete variate, such as fibrosis stages. Using our measurements of liver stiffness, spleen size, and platelet count obtained for our patients with CLD-B and CLD-C, we compared the degree of thrombocytopenia and splenomegaly with the adjustment for the degree of liver stiffness.

Patients and methods

Patients

A total of 245 consecutive patients with CLD-B or CLD-C who underwent liver stiffness measurements at the Department of Gastroenterology, University of Tokyo Hospital, Tokyo, Japan, between October 2006 and August 2009 were enrolled in this study. CLD-B was diagnosed based on positivity for hepatitis B surface antigen (HBsAg) for at least 6 months. CLD-C was defined by a positive result for serum anti-HCV antibodies and detectable HCV RNA. Exclusion criteria were co-infection of HBV and HCV, co-infection with human immunodeficiency virus, other causes of liver disease, and the existence of ascites, which hinders the liver stiffness measurement. The study was approved by the Institutional Research Ethics Committee of the Faculty of Medicine of the University of Tokyo.

Virological assays

HBsAg was measured using automated chemiluminescence enzyme immunoassay systems (Architect i2000; Abbott Laboratories Diagnostics, Abbott Park, IL) for HBsAg. Anti-HCV antibodies were measured by a third-generation enzyme immunoassay (Architect Anti-HCV; Abbott Laboratories Diagnostics). HCV RNA was assessed by qualitative (sensitivity, 50 IU/mL) or quantitative assays (Cobas Amplicore Hepatitis C Virus Test; Roche Diagnostics Systems, Branchburg, NJ).

Measurement of liver stiffness

Liver stiffness was measured by transient elastography (FibroScan 502; EchoSens, Paris, France) as described previously [22, 23, 27]. Briefly, the measurements were performed in the right lobe of the liver through the intercostal spaces with the patient lying in the dorsal decubitus position. The median value, calculated with at least ten successful acquisitions in each FibroScan examination, of which the success rate was more than 60%, was adopted and expressed in kilopascals (kPa). On the same day, the spleen size was measured, with the exception of patients with a previous splenectomy, using a common convex probe (3.75 MHz) with an ultrasound machine (SSA-770A Aplio XV; Toshiba Medical Systems, Tochigi, Japan). The spleen size was expressed as the splenic index, calculated as half the maximum craniocaudal

length multiplied by the maximum width of the spleen obtained on longitudinal sections [28].

Platelet count and biochemical assays

Platelet count was determined using a Coulter GEN-S System (Beckman Coulter, Miami, FL) in the clinical laboratory of the hospital. Serum alanine aminotransferase (ALT) activity, total bilirubin concentration, and albumin concentration were measured using an automated analyzer (Hitachi 7170; Hitachi Instruments Service Co, Tokyo, Japan). Prothrombin time was measured using an automated coagulometer (Coagrex 800; Sysmex Co, Kobe, Japan). For the purposes of this study, we adopted the laboratory data acquired on the same day as the liver stiffness measurement. Plasma thrombopoietin concentration was determined in plasma obtained on the day of the liver stiffness measurement, if any, by means of an enzyme-linked immunosorbent assay using a commercial kit (Quantikine Human TPO Immunoassay; R&D Systems, Minneapolis, MN); the reference range was 14–72 pg/mL in plasma [29].

Immature platelet fraction assay

A new automated method to reliably quantify reticulated platelets, expressed as the immature platelet fraction (IPF), was employed for this purpose; IPF was measured using the Sysmex XE-5000 automated hematology analyzer (Sysmex, Kobe, Japan) as previously described [30].

Statistical analysis

Data are expressed as medians with first to third quartile values (interquartile ranges; IQR). Between-group comparisons were made using Fisher's exact test, Mann–Whitney's U test, or an analysis of covariance (ANCOVA) where appropriate. The correlation between two groups, in which the data points were distribution-free, was analyzed using Spearman's rank correlation coefficient (rs). A two-sided P value <0.05 was considered to be statistically significant. Statistical procedures were performed using SAS ver. 9.1 (SAS Institute, Cary, NC).

Results

Patients

The characteristics of the enrolled 245 patients are summarized in Table 1. There were 102 patients with CLD-B and 143 patients with CLD-C. Relative to the CLD-C patients, the CLD-B patients were younger and there was a higher proportion of males. The comparison between the two groups without any adjustment revealed a significant difference in liver stiffness and platelet count, while there was no significant difference in spleen size. CLD-B patients also had a lower serum ALT activity and higher albumin concentration than CLD-C patients. When all of the patients were considered in the analysis, the strongest and most inverse correlation was found between liver stiffness and platelet count ($rs = -0.607$, $P < 0.001$), followed by serum albumin ($rs = -0.566$, $P < 0.001$), and prothrombin time ($rs = -0.505$, $P < 0.001$). There was also a strong correlation between liver stiffness and spleen size ($rs = 0.504$, $P < 0.001$), followed by serum ALT, and then by total bilirubin ($rs = 0.358$, 0.335, respectively, $P < 0.001$). Subsequently, a significant but weak correlation was observed between liver stiffness and age ($rs = 0.201$, $P = 0.002$), which may be explained by the evidence that liver fibrosis advances for a long period of time, especially in CLD-C. The distribution of liver stiffness values in patients with CLD-B and CLD-C is shown in Table 2.

Comparisons of platelet count between CLD-B and CLD-C patients

The possible difference in platelet count between CLD-B patients and CLD-C patients was first examined using ANCOVA to analyze the liver stiffness value, following logarithmic transformation because of its near log-normal distribution, as a covariate. The inter-group difference in platelet count was revealed to be significant ($P < 0.001$), while the interaction between the group and liver stiffness was not ($P = 0.845$). These results indicate that the platelet count is lower in CLD-C patients than in CLD-B patients when adjusted for the degree of liver stiffness.

We then compared platelet count between the two groups after stratification according to liver stiffness. We set four strata of liver stiffness values: first stratum, <5.0 kPa; second stratum, 5.0–10.0 kPa; third stratum, 10.0–15.0 kPa; fourth stratum, ≥15.0 kPa. These cut-off values were adopted from the distribution of liver stiffness values in the patients (Table 2) and also from previously published data showing 4.0–8.8, 9.5, and 11.9–17.6 kPa to be the lower limits of stages F2, F3, and F4, respectively, in the conventional classification of liver fibrosis [24, 31]. Platelet count was significantly higher in CLD-B patients than in CLD-C patients at both the highest and lowest stratum of liver stiffness (Fig. 1a).

Comparisons of spleen size between CLD-B and CLD-C patients

Spleen size was well correlated with liver stiffness in both CLD-B patients ($rs = 0.518$, $P < 0.001$) and CLD-C patients ($rs = 0.538$, $P < 0.001$), suggesting that spleen

Table 1 Characteristics of the 245 patients with chronic liver disease

	Total (n = 245)	HBV-related (n = 102)	HCV-related (n = 143)	HBV vs. HCV P value
Demographics				
Age (years)	61 (53–70)	55 (44–62)	66 (57–73)	<0.001[a]
Male:female	153:92	72:30	81:62	0.032[b]
Viral status				
HBsAg positive		102 [100]	0	
HCV-Ab positive		0	143 [100]	
HCV-RNA positive		Not tested	143 [100]	
Liver stiffness value (kPa)	8.6 (5.4–15.7)	7.8 (4.8–11.8)	10.0 (6.3–17.5)	0.004[a]
Platelet count ($\times 10^4$/mm^3)	15.0 (9.6–19.6)	16.9 (12.4–22.3)	13.5 (8.1–17.8)	<0.001[a]
Splenic index	15.8 (11.7–22.2)	16.0 (11.6–22.9)	15.6 (11.9–21.6)	0.581[a]
Biochemical markers				
ALT (IU/L)	32 (21–53)	27 (20–38)	38 (24–60)	<0.001[a]
Total bilirubin (mg/dL)	0.8 (0.7–1.1)	0.8 (0.6–1.1)	0.9 (0.7–1.3)	0.093[a]
Albumin (g/dL)	4.1 (3.8–4.3)	4.3 (4.0–4.5)	4.0 (3.6–4.2)	<0.001[a]
Prothrombin time (%)	83.1 (74.0–92.7)	84.4 (78.7–92.7)	81.3 (71.2–92.7)	0.070[a]

Data are given as the median with the first to third quartile values (interquartile range, IQR) in round parenthesis or as proportions (n) with the percentage in square parenthesis

Reference ranges: platelet count, 15.5–36.5 $\times$ 10^4/mm^3; splenic index, <20; serum ALT activity, 4–36 IU/L; total bilirubin concentration, 0.3–1.3 mg/dL; albumin concentration, 3.7–4.9 g/dL; prothrombin time, >70.0%

HCV, HBC, Hepatitis C, B; HBsAg, hepatitis B surface antigen; HCV-Ab, hepatitis C antibodies; ALT, alanine aminotransferase

P values <0.05 were considered to be significant

[a] The between-group comparison was made using Mann–Whitney's U test

[b] The between-group comparison was made using Fisher's exact test

Table 2 Distribution of liver stiffness values in patients with CLD-B and CLD-C

Liver stiffness value (kPa)	Patients with CLD-B[a]	Patients with CLD-C[a]	P value
<5.0	27 (26.5)	27 (18.9)	
	4.0 (3.5–4.4)	4.4 (3.7–4.5)	0.253
5.0≤, <10.0	44 (43.1)	44 (30.8)	
	7.5 (5.9–8.4)	7.4 (6.5–8.6)	0.701
10.0≤, <15.0	12 (11.8)	24 (16.8)	
	11.8 (11.8–12.5)	12.0 (11.0–14.0)	0.763
15.0≤	19 (18.6)	48 (33.6)	
	24.1 (20.1–25.6)	21.4 (17.5–27.7)	0.412
Total, n (%)	102 (100)	143 (100)	

CLD-B, -C, HBV- and HBC-related chronic liver disease, respectively

The between-group comparison of liver stiffness value in each stratum was made using Mann–Whitney's U test

[a] Data on liver stiffness are given in each cell as: top line, number (n) of patients, with the percentage in parenthesis; bottom line: median, with the IQR in parenthesis

size is similarly determined throughout the progression of liver stiffness in the two groups. A comparison of spleen size between CLD-B and CLD-C patients after stratification on liver stiffness revealed that spleen size was not significantly different between the two groups in any stratum of liver stiffness (Fig. 1b). Thus, the lower platelet count in the CLD-C patients of our study at the highest stratum of liver stiffness may not be explained by the increased platelet sequestration and destruction caused by splenomegaly.

Comparisons of biochemical markers between CLD-B and CLD-C patients

We then analyzed liver biochemical markers that were also adjusted for the degree of liver stiffness. As shown in

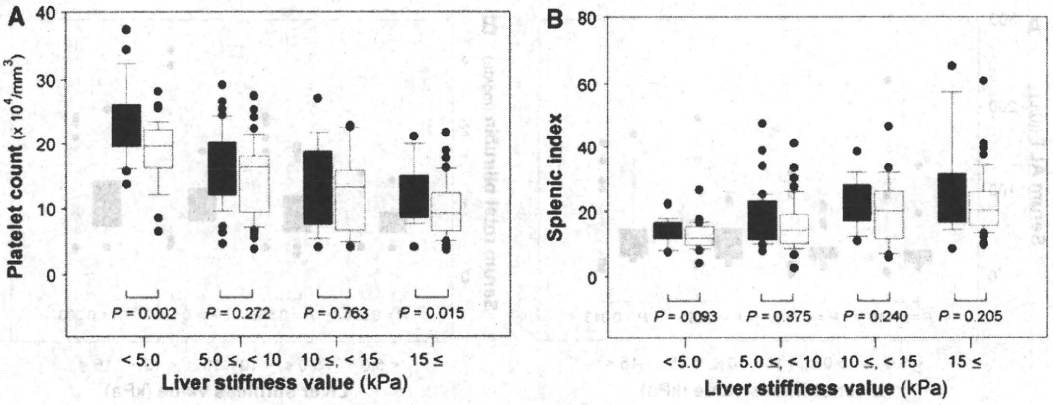

Fig. 1 Comparisons of platelet count or spleen size following stratification for liver stiffness between patients with chronic liver disease related to HBV (*CLD-B*) and HCV (*CLD-C*). Box plots of platelet count (**a**) and splenic index (**b**) in patients with CLD-B (*black boxes*) and CLD-C (*white boxes*). Thrombocytopenia and splenomegaly were defined as a platelet count $<15.5 \times 10^4/mm^3$ and a splenic index of >20, respectively. The *top* and *bottom* of the *boxes* represent the third and first quartile, respectively, with the *length* of the *box* therefore representing the inter-quartile range (IQR). The *horizontal lines inside* the *box* and the *error bars above* and *below* the *box* represent the median and 90th and 10th percentile values, respectively. The data points outside these ranges are also shown as *black dots*. Between-group comparisons were made using Mann–Whitney's *U* test. *P* values <0.05 were considered to be significant

Fig. 2a b, neither serum ALT activity nor total bilirubin concentration was significantly different between the CLD-B and CLD-C patients at any stratum of liver stiffness, including the stratum in which platelet count was different. Compared to CLD-C patients, CLD-B patients had higher serum albumin concentrations in the second to the fourth stratum (Fig. 2c) and higher prothrombin times (%) at the highest stratum of liver stiffness (Fig. 2d). These results suggest that the ability to produce proteins may be more highly impaired in CLD-C patients than in CLD-B patients.

Comparison of thrombopoietin levels between CLD-B and CLD-C patients

The data showing that the platelet count was significantly lower in CLD-C patients than in CLD-B patients at the highest stratum of liver stiffness led us to examine thrombopoietin level. It was possible to measure plasma thrombopoietin level in seven CLD-B patients and nine CLD-C patients at the highest stratum of liver stiffness. The liver stiffness values obtained, 22.6 (IQR 17.4–23.8) kPa and 21.5 (20.9–21.8) kPa in the CLD-B and CLD-C patients, respectively, were not significantly different between these two groups of patients ($P = 0.402$). The platelet count was significantly lower in CLD-C patients ($9.3 \times 10^4/mm^3$; IQR 7.2–10.2) than in CLD-B patients ($13.9 \times 10^4/mm^3$; 12.3–14.1) ($P = 0.007$). However, the plasma thrombopoietin levels in the studied patients were in lower part of the reference range—12.8 (IQR 4.0–15.6) pg/mL in CLD-B patients and 13.8 (6.5–35.5) pg/mL in CLD-C patients—and was not significantly different between the two groups ($P = 0.672$). The plasma thrombopoietin level is regulated by binding to platelets and megakaryocytes; consequently, a low platelet count is known to cause an increase in plasma thrombopoietin level due to a reduced binding to platelets [32–36]. As such, these results raise the possibility that thrombopoietin production may be more severely impaired in CLD-C patients than in CLD-B patients.

Comparison of IPF between CLD-B and CLD-C patients

To determine thrombopoietic activity in CLD-B and CLD-C patients, we also measured the IPF in 11 CLD-B and 13 CLD-C patients at the highest stratum of liver stiffness. IPF measurements have been recently employed to reliably quantify reticulated platelets, and IPF is considered to be a parameter of thrombopoietic activity in evaluating thrombocytopenia [30, 37]. In these 24 patients, the liver stiffness value was 17.6 (IQR 16.6–24.9) kPa in CLD-B patients and 20.9 (18.0–23.9) kPa in CLD-C patients; this difference is not significant ($P = 0.631$). The platelet count was significantly lower in CLD-C patients ($8.7 \times 10^4/mm^3$; IQR 6.1–10.3) than in CLD-B patients ($14.0 \times 10^4/mm^3$; 10.3–18.6) ($P = 0.002$); however, the IPF in CLD-C patients (3.8%; IQR 2.6–4.2) was not significantly higher than that in CLD-B patients (3.6%; 2.2–4.0) ($P = 0.930$). Of note, the number of immature platelets in CLD-C patients ($0.239 \times 10^4/mm^3$; IQR 0.187–0.400) was significantly lower than that in CLD-B patients ($0.396 \times 10^4/mm^3$; 0.373–0.435) ($P = 0.019$). These results suggest that thrombopoietic activity may be more severely impaired in CLD-C patients than in CLD-B patients.

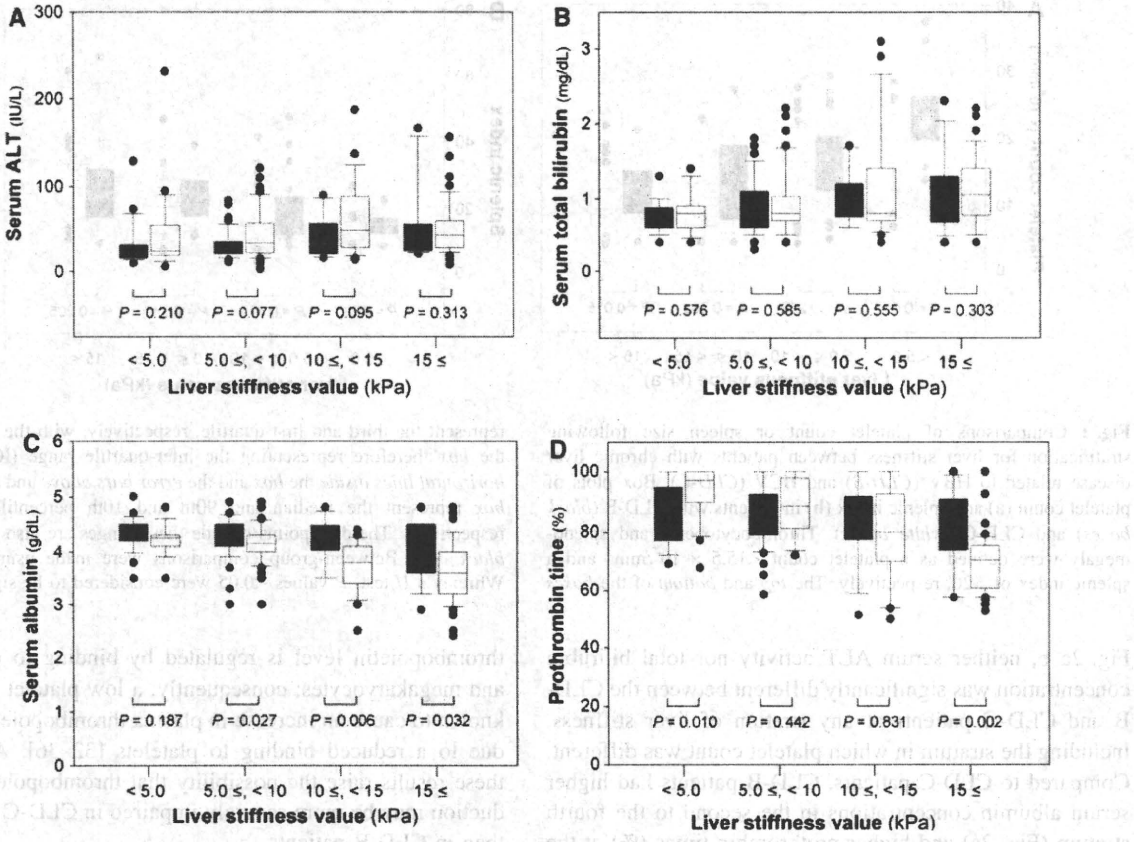

Fig. 2 Comparisons of biochemical markers following stratification for liver stiffness between patients with CLD-B and CLD-C. Box plots of serum alanine aminotransferase (ALT) activity (**a**), total bilirubin concentration (**b**), albumin concentration (**c**), and prothrombin time (**d**) in patients with CLD-B (*black boxes*) and CLD-C (*white boxes*). The *top* and *bottom* of the *boxes* represent the third and first quartile, respectively, with the *length* of the *box* therefore representing the IQR. The *horizontal lines inside* the *box* and the *error bars above* and *below* the *box* represent the median and 90th and 10th percentile values, respectively. The data points outside these ranges are also shown as *black dots*. Between-group comparisons were made using Mann–Whitney's *U* test. *P* values <0.05 were considered to be significant

Discussion

It has been reported that there is no difference in the platelet count between patients with cirrhosis related to HBV and HCV [38]. However, the data of that study were analyzed without stratification for the liver fibrosis stage, liver stiffness, or degree of splenomegaly. In contrast, we have shown here that thrombocytopenia was more severe in our CLD-C patients than in our CLD-B patients with stratification for high liver stiffness. The enrolled patients of the two groups differed in terms of the liver stiffness value, suggesting that the stage of CLD itself may be different. Therefore, in order to compare the severity of thrombocytopenia with adjusting the platelet count for the degree of liver stiffness, we performed ANCOVA and analyzed patients stratified for liver stiffness. Our ANCOVA, with liver stiffness as a covariate, revealed the lower platelet count in our CLD-C patients than in our CLD-B patients, indicating that liver stiffness and virological etiology independently affected the platelet count. In fact, CLD-C patients had a lower platelet count than CLD-B patients at the highest stratum of liver stiffness. These results suggest that virological etiology, namely, HBV or HCV, may distinctly contribute to thrombocytopenia in patients with advanced CLD.

The peripheral platelet count is regulated by the balance of its production and destruction. Because splenomegaly in CLD has been considered to cause thrombocytopenia by increased sequestration and enhanced destruction of platelets [6, 7], we asked the question of whether more splenomegaly may lead to a more severe form of thrombocytopenia in CLD-C patients than in CLD-B patients at the highest stratum of liver stiffness. However, the same degree of splenomegaly was determined at this stratum in both patients, suggesting that a specific mechanism(s) other than enhanced destruction caused by splenomegaly may be

at work to reduce platelet count. Spleen size was well correlated with liver stiffness and was same at all of the strata of liver stiffness between the two groups, suggesting that spleen size is similarly regulated throughout the progression of liver stiffness in CLD-B and CLD-C—unlike platelet count.

In addition to the difference in the degree of thrombocytopenia between CLD-B and CLD-C patients, serum albumin level and prothrombin time (%) were lower in the latter patient group after adjustment for liver stiffness, suggesting that the ability to produce proteins may be impaired more in CLD-C patients than CLD-B patients. Of note, thrombopoietin, an important regulator in platelet production [39–41], is known to be mainly produced in the liver [42]. Thrombopoietin has long been considered to play a role in the progression of thrombocytopenia in patients with CLD [43–46], but its exact role has not yet been clarified. It has been reported that the peripheral thrombopoietin level is correlated not only to the degree of liver fibrosis but also to liver functional impairment in patients with chronic viral hepatitis [10, 47–50], but conflicting findings have also been reported [51–54]. The plasma thrombopoietin level is mainly regulated by binding to platelets and megakaryocytes rather than by the upregulation or downregulation of its production [32–36]. For example, the plasma thrombopoietin level increases in patients with aplastic anemia or idiopathic thrombocytopenic purpura due to the reduced peripheral platelet count, with the increase being greater in aplastic anemia than idiopathic thrombocytopenic purpura because the megakaryocyte number is decreased in aplastic anemia. In our study, the number of immature platelets and the total platelet count were lower in CLD-C than in CLD-B patients at the highest stratum of liver stiffness. However, the plasma thrombopoietin level was not enhanced in any of these patients and was the same in both the CLD-C and CLD-B patients, suggesting that thrombopoietin production may be more severely impaired in CLD-C patients than in CLD-B patients. Collectively, these results suggest that the thrombopoietic activity may be impaired more in patients with CLD-C than in those with CLD-B. Of interest is the recent report that an active thrombopoietin-receptor agonist increased platelet counts in patients with HCV-related cirrhosis, thereby enabling the initiation of antiviral therapy and suggesting an important role of thrombopoietin in thrombocytopenia in advanced CLD-C patients [1].

It has recently been shown that transient elastography is an unreliable tool for the detection of cirrhosis in patients with acute liver damage [55] and that acute viral hepatitis increases liver stiffness values measured by transient elastography. These results suggest that the extent of necroinflammatory activity needs to be carefully considered in terms of validating transient elastography [55, 56]. In our study, the difference in liver damage assessed by ALT or total bilirubin was not determined in any stratum of liver stiffness of CLD-B and CLD-C patients, indicating that the evaluation of liver stiffness values was validated in all the strata of both patient groups. Regarding the potential influence of hepatitis viruses on the estimation of necroinflammatory activity by transient elastography, Marcellin et al. [57] recently reported that the liver stiffness measurement appears to be a reliable marker for the detection of significant fibrosis or cirrhosis in HBV patients and that cut-off values are only slightly different from those observed in HCV patients. In contrast, Ogawa et al. [58] showed that the liver stiffness cut-off value for each fibrosis stage was lower in patients with chronic HBV infection than in those with chronic HCV infection, indicating that the liver fibrosis stage may be higher in chronic HBV infection than in chronic HCV infection at the same stratum of liver stiffness. Whatever the case, there has been no report showing that liver fibrosis stage is more advanced in CLD-C than in CLD-B patients at the same liver stiffness, which could influence the results reported here. Furthermore, among CLD-B patients, the positivity of HBeAg may influence the liver stiffness measurement because patients with HBeAg are shown to have thicker fibrosis in portal area than those without HBeAg [59]. The significance of HBeAg positivity in the liver stiffness measurement should be further elucidated.

In conclusion, the data reported here indicate that the degree of thrombocytopenia is more severe in patients with advanced CLD-C than in those with CLD-B, even at the same grade of liver stiffness and splenomegaly, and that impaired platelet production may underlie the mechanism. The mechanism(s) responsible for thrombocytopenia—in addition to splenomegaly—in advanced CLD should be further elucidated with the aim of developing new therapeutic strategies.

References

1. McHutchison JG, Dusheiko G, Shiffman ML, Rodriguez-Torres M, Sigal S, Bourliere M, et al. Eltrombopag for thrombocytopenia in patients with cirrhosis associated with hepatitis C. N Engl J Med. 2007;357:2227–36.
2. National Institutes of Health. NIH Consensus Development Conference Statement: Management of hepatitis C. Hepatology. 2002;36:S3–20.
3. Poynard T, Yuen MF, Ratziu V, Lai CL. Viral hepatitis C. Lancet. 2003;362:2095–100.
4. Liaw YF, Tai DI, Chu CM, Chen TJ. The development of cirrhosis in patients with chronic type B hepatitis: a prospective study. Hepatology. 1988;8:493–6.
5. Fattovich G, Brollo L, Giustina G, Noventa F, Pontisso P, Alberti A, et al. Natural history and prognostic factors for chronic hepatitis type B. Gut. 1991;32:294–8.

6. Aster RH. Pooling of platelets in the spleen: role in the pathogenesis of "hypersplenic" thrombocytopenia. J Clin Invest. 1966;45:645–57.
7. Schmidt KG, Rasmussen JW, Bekker C, Madsen PE. Kinetics and in vivo distribution of 111-In-labelled autologous platelets in chronic hepatic disease: mechanisms of thrombocytopenia. Scand J Haematol. 1985;34:39–46.
8. Peck-Radosavljevic M. Hypersplenism. Eur J Gastroenterol Hepatol. 2001;13:317–23.
9. Bolognesi M, Merkel C, Sacerdoti D, Nava V, Gatta A. Role of spleen enlargement in cirrhosis with portal hypertension. Dig Liver Dis. 2002;34:144–50.
10. Adinolfi LE, Giordano MG, Andreana A, Tripodi MF, Utili R, Cesaro G, et al. Hepatic fibrosis plays a central role in the pathogenesis of thrombocytopenia in patients with chronic viral hepatitis. Br J Haematol. 2001;113:590–5.
11. Karasu Z, Tekin F, Ersoz G, Gunsar F, Batur Y, Ilter T, et al. Liver fibrosis is associated with decreased peripheral platelet count in patients with chronic hepatitis B and C. Dig Dis Sci. 2007;52:1535–9.
12. Lu SN, Wang JH, Liu SL, Hung CH, Chen CH, Tung HD, et al. Thrombocytopenia as a surrogate for cirrhosis and a marker for the identification of patients at high-risk for hepatocellular carcinoma. Cancer. 2006;107:2212–22.
13. Imbert-Bismut F, Ratziu V, Pieroni L, Charlotte F, Benhamou Y, Poynard T. Biochemical markers of liver fibrosis in patients with hepatitis C virus infection: a prospective study. Lancet. 2001;357:1069–75.
14. Myers R, Tainturier M, Ratziu V, Piton A, Thibault V, Imbert-Bismut F, et al. Prediction of liver histological lesions with biochemical markers in patients with chronic hepatitis B. J Hepatol. 2003;39:222–30.
15. Yeh WC, Li PC, Jeng YM, Hsu HC, Kuo PL, Li ML, et al. Elastic modulus measurements of human liver and correlation with pathology. Ultrasound Med Biol. 2002;28:467–74.
16. Saito H, Tada S, Nakamoto N, Kitamura K, Horikawa H, Kurita S, et al. Efficacy of non-invasive elastometry on staging of hepatic fibrosis. Hepatol Res. 2004;29:97–103.
17. Dienstag J. The role of liver biopsy in chronic hepatitis C. Hepatology. 2002;36:S152–60.
18. Lok A, McMahon B. Chronic hepatitis B. Hepatology. 2001;34:1225–41.
19. Maharaj B, Maharaj R, Leary W, Cooppan R, Naran A, Pirie D, et al. Sampling variability and its influence on the diagnostic yield of percutaneous needle biopsy of the liver. Lancet. 1986;1:523–5.
20. McGill D, Rakela J, Zinsmeister A, Ott B. A 21-year experience with major hemorrhage after percutaneous liver biopsy. Gastroenterology. 1990;99:1396–400.
21. Sandrin L, Fourquet B, Hasquenoph JM, Yon S, Fournier C, Mal F, et al. Transient elastography: a new noninvasive method for assessment of hepatic fibrosis. Ultrasound Med Biol. 2003;29:1705–13.
22. Castera L, Vergniol J, Foucher J, Le Bail B, Chanteloup E, Haaser M, et al. Prospective comparison of transient elastography, Fibrotest, APRI, and liver biopsy for the assessment of fibrosis in chronic hepatitis C. Gastroenterology. 2005;128:343–50.
23. Ziol M, Handra-Luca A, Kettaneh A, Christidis C, Mal F, Kazemi F, et al. Noninvasive assessment of liver fibrosis by measurement of stiffness in patients with chronic hepatitis C. Hepatology. 2005;41:48–54.
24. Verveer C, de Knegt RJ. Non-invasive measurement of liver fibrosis: application of the FibroScan in hepatology. Scand J Gastroenterol. 2006;41[Suppl 243]:85–8.
25. Ganne-Carrie N, Ziol M, de Ledinghen V, Douvin C, Marcellin P, Castera L, et al. Accuracy of liver stiffness measurement for the diagnosis of cirrhosis in patients with chronic liver diseases. Hepatology. 2006;44:1511–7.
26. Fraquelli M, Rigamonti C. Diagnosis of cirrhosis by transient elastography: what is hidden behind misleading results. Hepatology 2007;46:282 (author reply, p. 283).
27. Masuzaki R, Tateishi R, Yoshida H, Yoshida H, Sato S, Kato N, et al. Risk assessment of hepatocellular carcinoma in chronic hepatitis C patients by transient elastography. J Clin Gastroenterol. 2008;42:839–43.
28. Lamb PM, Lund A, Kanagasabay RR, Martin A, Webb JA, Reznek RH. Spleen size: how well do linear ultrasound measurements correlate with three-dimensional CT volume assessments? Br J Radiol. 2002;75:573–7.
29. Kurata Y, Hayashi S, Kiyoi T, Kosugi S, Kashiwagi H, Honda S, et al. Diagnostic value of tests for reticulated platelets, plasma glycocalicin, and thrombopoietin levels for discriminating between hyperdestructive and hypoplastic thrombocytopenia. Am J Clin Pathol. 2001;115:656–64.
30. Briggs C, Kunka S, Hart D, Oguni S, Machin SJ. Assessment of an immature platelet fraction (IPF) in peripheral thrombocytopenia. Br J Haematol. 2004;126:93–9.
31. Cobbold JF, Morin S, Taylor-Robinson SD. Transient elastography for the assessment of chronic liver disease: Ready for the clinic? World J Gastroenterol. 2007;13:4791–7.
32. Bartley TD, Bogenberger J, Hunt P, Li YS, Lu HS, Martin F, et al. Identification and cloning of a megakaryocyte growth and development factor that is a ligand for the cytokine receptor Mpl. Cell. 1994;77:1117–24.
33. Kaushansky K, Lok S, Holly RD, Broudy VC, Lin N, Bailey MC, et al. Promotion of megakaryocyte progenitor expansion and differentiation by the c-Mpl ligand thrombopoietin. Nature. 1994;369:568–71.
34. Fielder PJ, Gurney AL, Stefanich E, Marian M, Moore MW, Carver-Moore K, et al. Regulation of thrombopoietin levels by c-mpl-mediated binding to platelets. Blood. 1996;87:2154–61.
35. Emmons RV, Reid DM, Cohen RL, Meng G, Young NS, Dunbar CE, et al. Human thrombopoietin levels are high when thrombocytopenia is due to megakaryocyte deficiency and low when due to increased platelet destruction. Blood. 1996;87:4068–71.
36. Li J, Xia Y, Kuter DJ. Interaction of thrombopoietin with the platelet c-mpl receptor in plasma: binding, internalization, stability and pharmacokinetics. Br J Haematol. 1999;106:345–56.
37. Koike Y, Miyazaki K, Higashihara M, Kimura E, Jona M, Uchihashi K, et al. Clinical significance of detection of immature platelets: comparison between percentage of reticulated platelets as detected by flow cytometry and immature platelet fraction as detected by automated measurement. Eur J Haematol. 2010;84:183–4.
38. Kajihara M, Okazaki Y, Kato S, Ishii H, Kawakami Y, Ikeda Y, et al. Evaluation of platelet kinetics in patients with liver cirrhosis: similarity to idiopathic thrombocytopenic purpura. J Gastroenterol Hepatol. 2007;22:112–8.
39. Kaushansky K. Thrombopoietin: basic biology, clinical promise. Int J Hematol. 1995;62:7–15.
40. Kaushansky K. Thrombopoietin: the primary regulator of megakaryocyte and platelet production. Thromb Haemost. 1995;74:521–5.
41. Eaton DL, de Sauvage FJ. Thrombopoietin: the primary regulator of megakaryocytopoiesis and thrombopoiesis. Exp Hematol. 1997;25:1–7.
42. Jelkmann W. The role of the liver in the production of thrombopoietin compared with erythropoietin. Eur J Gastroenterol Hepatol. 2001;13:791–801.

43. Koike Y, Yoneyama A, Shirai J, Ishida T, Shoda E, Miyazaki K, et al. Evaluation of thrombopoiesis in thrombocytopenic disorders by simultaneous measurement of reticulated platelets of whole blood and serum thrombopoietin concentrations. Thromb Haemost. 1998;79:1106–10.
44. Peck-Radosavljevic M, Wichlas M, Zacherl J, Stiegler G, Stohlawetz P, Fuchsjager M, et al. Thrombopoietin induces rapid resolution of thrombocytopenia after orthotopic liver transplantation through increased platelet production. Blood. 2000;95:795–801.
45. Peck-Radosavljevic M. Thrombocytopenia in liver disease. Can J Gastroenterol. 2000;14[Suppl D]:60D–6D.
46. Wolber EM, Ganschow R, Burdelski M, Jelkmann W. Hepatic thrombopoietin mRNA levels in acute and chronic liver failure of childhood. Hepatology. 1999;29:1739–42.
47. Kawasaki T, Takeshita A, Souda K, Kobayashi Y, Kikuyama M, Suzuki F, et al. Serum thrombopoietin levels in patients with chronic hepatitis and liver cirrhosis. Am J Gastroenterol. 1999;94:1918–22.
48. Espanol I, Gallego A, Enriquez J, Rabella N, Lerma E, Hernandez A, et al. Thrombocytopenia associated with liver cirrhosis and hepatitis C viral infection: role of thrombopoietin. Hepatogastroenterology. 2000;47:1404–6.
49. Giannini E, Borro P, Botta F, Fumagalli A, Malfatti F, Podesta E, et al. Serum thrombopoietin levels are linked to liver function in untreated patients with hepatitis C virus-related chronic hepatitis. J Hepatol. 2002;37:572–7.
50. Giannini E, Botta F, Borro P, Malfatti F, Fumagalli A, Testa E, et al. Relationship between thrombopoietin serum levels and liver function in patients with chronic liver disease related to hepatitis C virus infection. Am J Gastroenterol. 2003;98:2516–20.
51. Stockelberg D, Andersson P, Bjornsson E, Bjork S, Wadenvik H. Plasma thrombopoietin levels in liver cirrhosis and kidney failure. J Intern Med. 1999;246:471–5.
52. Schoffski P, Tacke F, Trautwein C, Martin MU, Caselitz M, Hecker H, et al. Thrombopoietin serum levels are elevated in patients with hepatitis B/C infection compared to other causes of chronic liver disease. Liver. 2002;22:114–20.
53. Aref S, Mabed M, Selim T, Goda T, Khafagy N. Thrombopoietin (TPO) levels in hepatic patients with thrombocytopenia. Hematology. 2004;9:351–6.
54. Ozer B, Serin E, Sezgin N, Cosar A, Guclu M, Gur G, et al. Thrombopoietin or interleukin-6 has no effect on thrombocytopenia of cirrhosis. Hepatogastroenterology. 2007;54:1187–91.
55. Sagir A, Erhardt A, Schmitt M, Haussinger D. Transient elastography is unreliable for detection of cirrhosis in patients with acute liver damage. Hepatology. 2008;47:592–5.
56. Arena U, Vizzutti F, Corti G, Ambu S, Stasi C, Bresci S, et al. Acute viral hepatitis increases liver stiffness values measured by transient elastography. Hepatology. 2008;47:380–4.
57. Marcellin P, Ziol M, Bedossa P, Douvin C, Poupon R, de Ledinghen V, et al. Non-invasive assessment of liver fibrosis by stiffness measurement in patients with chronic hepatitis B. Liver Int. 2009;29:242–7.
58. Ogawa E, Furusyo N, Toyoda K, Takeoka H, Otaguro S, Hamada M, et al. Transient elastography for patients with chronic hepatitis B and C virus infection: non-invasive, quantitative assessment of liver fibrosis. Hepatol Res. 2007;37:1002–10.
59. Hui CK, Leung N, Shek TW, Yao H, Lee WK, Lai JY, et al. Sustained disease remission after spontaneous HBeAg seroconversion is associated with reduction in fibrosis progression in chronic hepatitis B Chinese patients. Hepatology. 2007;46:690–8.

Expression of α-taxilin in hepatocellular carcinoma correlates with growth activity and malignant potential of the tumor

NATSUKO OHTOMO[1], TOMOAKI TOMIYA[1], YASUSHI TANOUE[1], YUKIKO INOUE[1], TAKAKO NISHIKAWA[1], HITOSHI IKEDA[4], YASUJI SEYAMA[2], NORIHIRO KOKUDO[2], JUNJI SHIBAHARA[3], MASASHI FUKAYAMA[3], KAZUHIKO KOIKE[1], HIROMICHI SHIRATAKI[5] and KENJI FUJIWARA[6]

Departments of [1]Gastroenterology, [2]Hepato-Biliary-Pancreatic Surgery and [3]Pathology, University of Tokyo; [4]Clinical Laboratory, University of Tokyo Hospital, 7-3-1 Hongo, Bunkyo-ku, Tokyo; [5]Molecular and Cell Biology, Dokkyo Medical School, 880 Kitakobayashi, Mibu-machi, Shimotsuga-gun, Tochigi; [6]Yokohama Rosai Hospital, 3211 Kodukue-cho, Kohoku-ku, Yokohama, Kanagawa, Japan

DOI: 10.3892/ijo_xxxxxxxx

Abstract. The membrane traffic system has been recognized to be involved in carcinogenesis and tumor progression in several types of tumors. α-taxilin is a newly identified membrane traffic-related molecule, and its up-regulation has been reported in embryonic and malignant tissues of neural origin. In the present study, we analyzed the expression of α-taxilin in relation to clinicopathological features of hepatocellular carcinomas (HCC) and proliferative activity of the tumor determined by proliferating cell nuclear antigen labeling index (PCNA-LI). Twenty-nine surgically resected nodules of HCC (8 well-, 11 moderately-, and 10 poorly-differentiated) were studied. Fifteen cases showed 'strong staining', while 14 cases showed 'weak staining' for α-taxilin. A significantly higher expression of α-taxilin was observed in less-differentiated (p=0.005), and more invasive (p=0.016) HCCs. The 'strong staining' group showed significantly higher PCNA-LI than the 'weak staining' group (the medians of PCNA-LI were 59.4% vs. 14.4%, p<0.0001). We also evaluated the expression of α-taxilin in hepatoma cell lines (PLC/PRF/5, Hep G2 and HuH-6) in association with cell proliferation. The expression levels of α-taxilin protein were correlated with their growth rates. In conclusion, the expression of the α-taxilin protein was related with an increased proliferative activity and a less-differentiated histological grade of HCC. α-taxilin may be involved in cell proliferation of HCC, and its expression can be a marker of malignant potential of HCC.

Correspondence to: Dr Tomoaki Tomiya, Department of Gastroenterology, University of Tokyo, 7-3-1 Hongo, Bunkyo-ku, Tokyo, Japan
E-mail: tomiya-1im@h.u-tokyo.ac.jp

Key words: hepatocellular carcinoma, taxilin, vesicular transport proteins

Introduction

The molecular mechanisms of carcinogenesis and tumor progression have been extensively investigated to find novel targets for anti-tumor therapy as well as useful predictors of tumor growth and biological aggressiveness. Involvement of intracellular signaling pathways, cell cycle regulators, growth factors and angiogenic factors has been shown in a variety of carcinomas (1,2). Furthermore, recent studies have revealed that membrane traffic-related molecules play a role in the processes of carcinogenesis and tumor progression in several types of tumors (3-5).

Membrane traffic is a fundamental intracellular transport system in eukaryotic cells (6). Small transport vesicles bud from membranes of a donor compartment, and subsequently fuse with membranes of a target compartment. Cargo molecules in the vesicles as well as biomembranes are dynamically exchanged between organelles with temporal and spatial selectivity. These processes are essential for multiple cellular functions such as endo- and exocytosis, maintenance of organelle homeostasis and cell growth, division, and motility. Soluble *N*-ethylmaleimide-sensitive factor attachment protein receptors (SNAREs), located on vesicles and the target membranes, are the central coordinators of membrane traffic (7), and syntaxin family proteins are their main components.

Recently, taxilin was identified as a novel binding partner of syntaxins (8). α-taxilin, one of the isoforms, was proposed to be involved in Ca^{++}-dependent exocytosis in neuroendocrine cells, although its actual function *in vivo* is not yet known. Over-expression of *α-taxilin* mRNA has been reported in human glioblastoma compared to normal tissues of the central nervous system (CNS) (9). Prominent up-regulation of α-taxilin protein has also been reported in proliferating neural stem cells during embryonic development in rats followed by a rapid decrease of the expression level as development proceeds (10). These findings imply that α-taxilin is related to cell proliferation of mesenchymal cells, especially in the CNS. However, significance of the expression of α-taxilin protein has not yet been studied in tissues or malignancies of epithelial origin.

In the present study, we analyzed the expression of α-taxilin in hepatocellular carcinomas (HCC), which is one of the most common malignancies of epithelial origin worldwide and is known to have wide varieties of differentiation and growth activity. We found a correlation of α-taxilin expression with proliferative activity as well as with malignant potential of HCC.

Patients and methods

Patients. Twenty-nine patients of HCC were studied who underwent curative or non-curative hepatectomy at the Hepato-Biliary-Pancreatic and Transplantation Division between May 2003 and August 2008. No patients received preoperative treatments for HCC. Diagnosis of HCC was confirmed by histology based on sections stained with hematoxylin and eosin. The degree of tumor differentiation and other pathological features were assessed according to the Liver Cancer Study Group of Japan (11), and reviewed by a pathologist who was not informed of the results of α-taxilin expression. When there were multiple nodules of HCC in the resected tissues, the largest one was considered to be representative. The clinical and pathological features of the study population are shown in Table I. Informed consent was obtained from each participant. This study protocol was approved by the institutional review board of the University of Tokyo.

Immunohistochemistry of α-taxilin. The polyclonal anti-human α-taxilin antibody raised in a rabbit was used for immunohistochemistry, as previously described (12).

The formalin-fixed, paraffin-embedded liver specimens containing HCC nodules were sliced into 3 μm-thick sections, immersed in xylene and graded alcohols, and washed in 10 mM PBS. The sections were heated using a microwave processor MI-77 (Azumaya, Tokyo, Japan) in 10 mM citrate buffer (pH 6.0) at 95˚C for 30 min. The sections were treated with 0.3% v/v H_2O_2 in methanol at room temperature for 30 min, blocking solution (10% v/v normal goat serum and 1% w/v BSA in 10 mM PBS) at room temperature for 1 h, and then incubated with a primary antibody diluted in the blocking solution overnight at 4˚C.

A standard avidin-biotin-peroxidase complex (ABC) technique with Vectastain® ABC elite kit (Vector Laboratories, Burlingame, CA, USA) was applied. Briefly, a biotinylated antibody against rabbit IgG diluted in the blocking solution and ABC solution were applied at room temperature for 25 and 30 min, respectively. Staining was visualized with 3,3'-diaminobenzidine working solution (Vector Laboratories) with nuclear counterstaining in Mayer's hematoxylin (Wako Pure Chemical Industries Ltd., Osaka, Japan).

The sections were studied with a light microscope Eclipse 80i (Nikon, Tokyo, Japan) at magnifications x40, x100 and x200 with a digital camera DXM1200F (Nikon). Intensity of α-taxilin staining was evaluated independently by three of the authors. The intensity of staining in HCC tissues was classified into two categories: 'strong staining' where almost all the cancerous cells were stained (Fig. 1A), and 'weak staining' where no stained cells or few weakly stained cells were observed in cancerous tissues (Fig. 1B).

Immunohistochemistry of proliferating cell nuclear antigen (PCNA) in HCC. Immunohistochemistry of PCNA was performed on the serial section of the specimens as mentioned above except for blocking solution (10% v/v normal horse serum and 1% w/v BSA in 10 mM PBS), the primary antibody (mouse monoclonal anti-PCNA antibody (clone PC10; dilution 1:200; Dako, Glostrup, Denmark)), the secondary antibody (a biotinylated anti-mouse IgG) and the duration of microwave heating (10 min).

PCNA labeling index (PCNA-LI) was determined by random evaluation of at least 1,000 HCC cell nuclei at magnification x100. All of the stained nuclei were regarded as positive. PCNA-LI was expressed as the percentage of positive nuclei (13,14).

Preparation of frozen tissue samples of HCC for Western blotting. Western blotting was performed on fresh frozen tissue samples from one representative case showing 'strong staining' of α-taxilin. The samples obtained at hepatectomy from the HCC nodule and adjacent non-cancerous liver tissue were snap-frozen in liquid nitrogen, and stored at -80˚C. They were homogenized in ice-cold buffer containing 20 mM Tris/HCl (pH 7.5), 150 mM NaCl, 1 mM EDTA, Protease inhibitor cocktail Complete® (Roche Diagnostics, Basel, Switzerland), 1 mM DTT, and 2% w/v Triton X-100, incubated for 1 h with intermittent vortexing.

Preparation of lysates of hepatoma cell lines for Western blotting. The human hepatoma cell lines, Hep G2 (cell no. JCRB1054), PLC/PRF/5 (JCRB0406) and HuH-6 Clone 5 (JCRB0401) were purchased from Health Science Research Resources Bank (Osaka, Japan) in November 2008. The cell lines were authorized by Multiplex PCR method using short tandem repeat by the cell bank.

The cells were plated on plastic culture dishes (BD, Franklin Lakes, NJ, USA) at a density of 3,000 cells/cm^2 in DMEM with 10% v/v FCS and grown to 50-70% confluency. The cells were lysed in ice-cold buffer containing 50 mM Tris/HCl (pH 8.0), 120 mM NaCl, 20 mM NaF, 1 mM EDTA, 6 mM EGTA, 0.5 mM DTT, protease inhibitor cocktail, and 1% v/v NP-40, incubated for 10 min with intermittent vortexing.

Western blotting for α-taxilin. Protein concentrations of the tissue homogenates and the cell lysates were determined by the Lowry's method with DC™ protein assay kit (Bio-Rad Laboratories, Hercules, CA, USA). The samples were adjusted to the same protein concentration, boiled at 95˚C for 5 min with a half volume of SDS buffer (186 mM Tris/HCl (pH 6.7), 9% SDS, 15% glycerol, 6% 2-mercaptoethanol, bromophenol blue), separated by SDS-PAGE on a 10% polyacrylamide gel, and transferred to PVDF membranes (GE Healthcare, Buckinghamshire, UK). The membranes were treated with blocking buffer (10 mM PBS containing 5% w/v skim milk and 0.1% w/v Tween-20) for 1 h at room temperature, and incubated with 0.1 μg/ml of anti-human α-taxilin antibody in the blocking buffer overnight at 4˚C, and subsequently with HRP-conjugated anti-rabbit IgG (GE Healthcare) in the blocking buffer (dilution 1:2,000) for 45 min at room temperature. The chemiluminescent signals were visualized

Table I. α-taxilin expression in HCC and clinical and pathological features.

		Intensity of α-taxilin expression		
	All	Weak (%)	Strong (%)	P-value
Age[a]	68.0 (45-76)	68.0 (51-76)	68.0 (45-76)	
<68	14	7 (50)	7 (50)	0.860
≥68	15	7 (47)	8 (53)	
Gender				
Male	24	10 (42)	14 (58)	0.125
Female	5	4 (80)	1 (20)	
Background liver[b]				
Liver cirrhosis	17	10 (59)	7 (41)	0.395
Chronic hepatitis	10	4 (40)	6 (60)	
Normal liver	1	0 (0)	1(100)	
Number of tumors				
Solitary	20	10 (50)	10 (50)	0.786
Multifocal	9	4 (44)	5 (56)	
Tumor diameter cm)[a]	3.0 (0.9-7.5)	2.6 (1-5.5)	3.7 (0.9-7.5)	
<3.0	15	9 (60)	6 (40)	0.199
≥3.0	14	5 (36)	9 (64)	
Degree of tumor differentiation				
Well	8	7 (88)	1 (12)	0.005
Moderately	11	6 (55)	5 (45)	
Poorly	10	1 (10)	9 (90)	
Tumor invasiveness (vascular invasion and/or intrahepatic metastasis)				
Negative	16	11 (69)	5 (31)	0.016
Positive	13	3 (23)	10 (77)	
Fibrous capsular formation/infiltration				
Negative	11	3 (27)	8 (73)	0.216
Positive/negative	3	2 (67)	1 (33)	
Positive/positive	15	9 (60)	6 (40)	

Data shown are number of cases, and the numbers in parenthesis are percentage of cases unless otherwise indicated. [a]Data are expressed as median (range). [b]Data are not available in 1 case.

with ECL plus™ (GE Healthcare) and detected by LAS-1000 (Fujifilm, Tokyo, Japan).

Cell proliferation assay. The human hepatoma cell lines mentioned above were seeded into 96-well tissue culture plates (BD) at 1,000 cells/well in DMEM supplemented with 10% v/v FCS. After 24, 48 and 72 h, the numbers of viable cells were determined by a soluble tetrazolium/formazan assay using Cell Counting Kit-8 (Dojindo Laboratories, Kumamoto, Japan) (15).

Statistical analysis. Statistical analysis was performed using StatView 5.0J software (SAS Institute Inc., Cary, NC, USA). The Mann-Whitney U test was performed to compare variables of two categories. The Kruskal-Wallis test followed by the Scheffé's *post hoc* test was performed to compare variables of three or more categories. All statistical analyses were considered to be significant at $p<0.05$.

Results

Immunohistochemical staining of α-taxilin in HCCs and non-cancerous liver tissues. Diffuse granular staining of α-taxilin was observed in the cytoplasm of HCC cells. Fifteen cases were classified as 'strong staining', where all the tumor cells

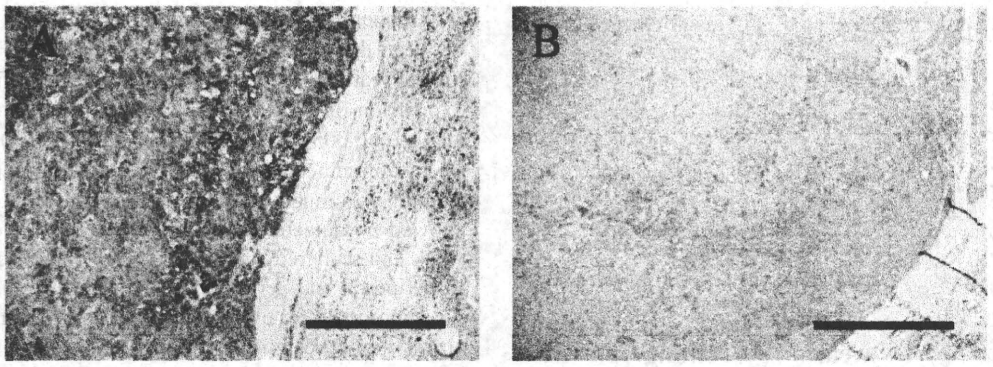

Figure 1. Expression of α-taxilin in HCCs. Intensities of staining were classified into 2 categories: (A) strong staining, almost all the cancerous cells were stained; (B) weak staining, no stained cells or few weakly stained cells were observed in cancerous tissues. Bar, 200 μm.

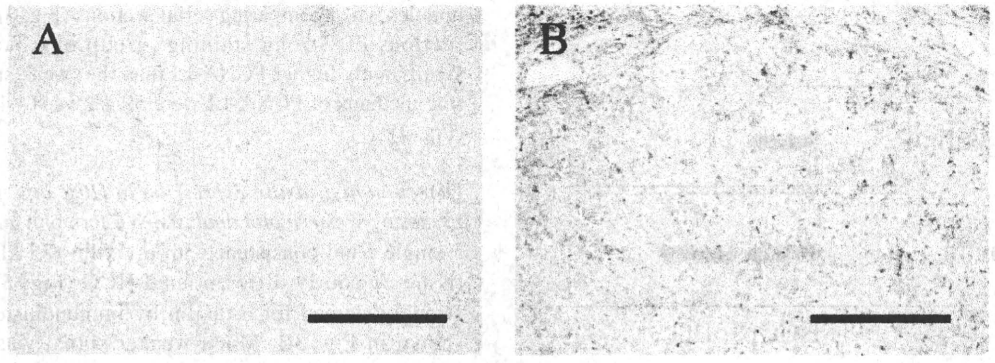

Figure 2. Expression of α-taxilin in non-cancerous tissues. Intensities of staining were evaluated as undetectable (A), or weakly detectable (B). Bar, 200 μm.

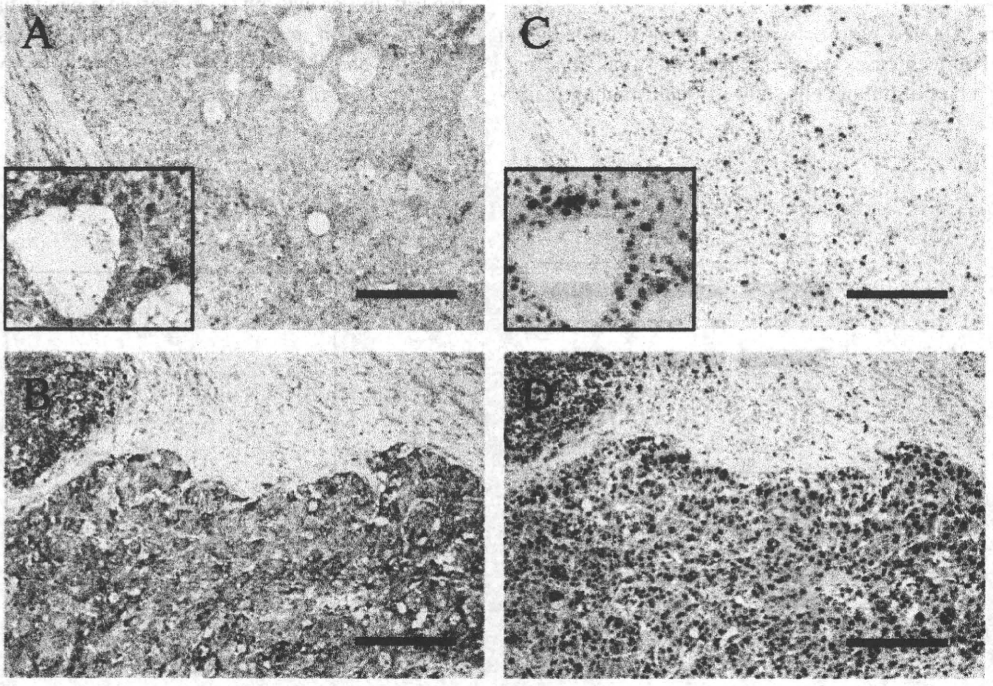

Figure 3. Expression of α-taxilin (A and B) and PCNA (C and D) in HCCs. Intensities of α-taxilin staining and PCNA-LI were determined in serial sections. Two representative cases are shown. Case 1, weak staining of α-taxilin (A) and 7.5% of PCNA-LI (C). Case 2, strong staining of α-taxilin (B) and 94.2% of PCNA-LI (D). Magnified pictures are shown in boxes (A and C). Bar, 500 μm.

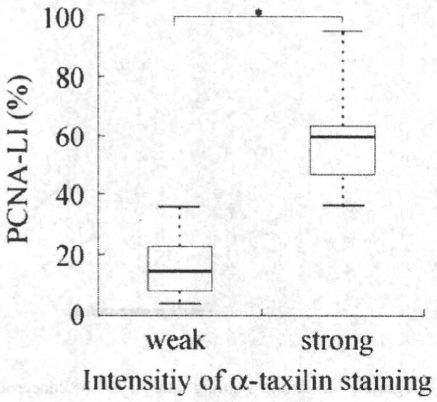

Figure 4. Relationship between α-taxilin expression and PCNA-LI. Tukey's box-and whisker plot are shown. Asterisk indicates a significant difference ($p<0.0001$ by the Mann-Whitney U test).

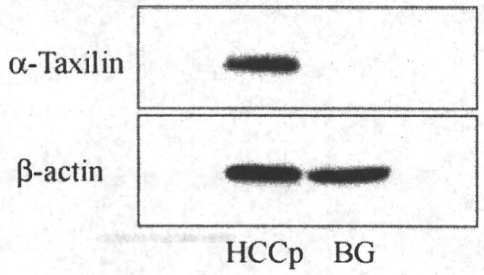

Figure 5. Expression of α-taxilin in HCC and surrounding non-cancerous liver tissue, determined by Western blotting. HCCp, cancerous tissue obtained from poorly differentiated HCC; BG, non-cancerous background liver tissue.

were clearly stained with or without strongly stained foci (Fig. 1A). Fourteen cases were classified as 'weak staining', where only a part of tumor cells showed weak staining mainly in periphery of the tumor nodules (Fig. 1B). Relationships between the α-taxilin expression and various clinicopathological features were shown in Table I. Significantly higher expression of α-taxilin was observed in less differentiated HCCs ($p=0.005$), and more invasive HCCs ($p=0.016$).

In non-cancerous liver tissues surrounding HCCs, the staining was much weaker compared to HCCs. Eleven cases showed no detectable staining (Fig. 2A), 17 cases showed weak and scattered staining in the cytoplasm of hepatocytes in periportal and periseptal areas (Fig. 2B), and 1 case was not appropriate for evaluation because of the small specimen size of non-cancerous tissue.

Relationship between expressions of α-taxilin and PCNA in HCCs. PCNA-LI in HCCs ranged from 3.4 to 94.2%, and the median was 36.0%. α-taxilin-positive cells and PCNA-positive cells showed very similar distribution in the tumor nodules when comparing serial sections (Fig. 3A and C). The sections of 'strong staining' group of α-taxilin showed significantly higher PCNA-LI than the 'weak staining' group (the medians of PCNA-LI were 59.4% vs. 14.4%, $p<0.0001$) (Fig. 4).

Detection of α-taxilin expression in HCC and non-cancerous tissues by Western blot analysis. Western blot analysis showed a single band consistent with α-taxilin (75 kDa) (8) in the tissue of poorly differentiated HCC (Fig. 5), which was strongly stained for α-taxilin by immunohistochemistry as shown in Fig. 3B. Much weaker signal was detected by Western blotting in the surrounding non-cancerous tissue.

Relationship between α-taxilin expression and cellular proliferation in hepatoma cell lines. All the cell lines in logarithmic-growth phase expressed a single band consistent with α-taxilin at various intensities by Western blotting (Fig. 6A and B). The rate of cell growth correlated with the intensity of α-taxilin expression (Fig. 6C).

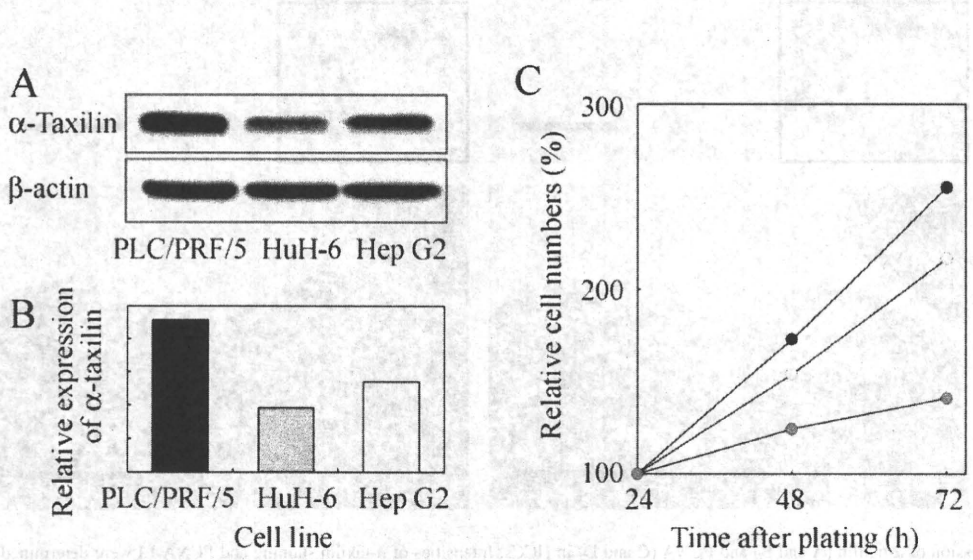

Figure 6. Expression of α-taxilin in hepatoma cell lines (A and B) and cell proliferation rate (C). Closed circles, open circles and shaded circles indicate PLC/PRF/5, Hep G2 and HuH-6, respectively. The expression levels of α-taxilin in the cell lines were correlated with their growth rates.

Discussion

We demonstrated the expression of α-taxilin in HCCs, and its expression levels correlated with dedifferentiation, invasiveness and growth activity. We used a rabbit polyclonal anti-human α-taxilin antibody. Previous reports have shown a single band in lysates of HeLa and COS-7 cells expressing human recombinant α-taxilin by Western blotting using this antibody (12). In the present study, a similar single band consistent with α-taxilin molecular weight was detected in HCC specimen and hepatoma cell lines by Western blotting. This antibody detects α-taxilin specifically in HCC cells.

We determined proliferative activity of HCC using PCNA-LI. PCNA accumulates in the nuclei during S-phase of the cell cycle (16), and is considered as a marker of proliferative activity of various tumors including HCC (13,14,17-20). Previous studies have reported that PCNA-LI in HCCs ranged from 0.2 to 73.3% (13), from 1.0 to 89.4% (17), and from 1.2 to 91.6% (18). In the present study, PCNA-LI was ranged from 3.9 to 94.2%, which is in line with previous reports. The grade of α-taxilin expression in HCCs showed a significant positive correlation with PCNA-LI. In addition, the spatial distribution of α-taxilin positive cells was similar with that of PCNA. These findings suggest that expression levels of α-taxilin relate to proliferative activity of HCC. This notion is supported by the data of *in vitro* experiments showing the relationship between the extent of α-taxilin and proliferative activity of hepatoma cell lines.

Enhanced α-taxilin expression in HCCs was also significantly correlated with less-differentiated histological grade, and more invasive characteristics indicated by positivity for vascular invasion and/or intrahepatic metastasis (21,22). Dedifferentiation of HCCs is usually considered to be associated with higher proliferative activity of the tumor and higher risk of vascular invasion and metastases (2). In addition, in the 'weak staining' cases, α-taxilin positive cells tended to distribute in the periphery of tumor nodules. This feature is also reported for several proteins associated with tumor progression and angiogenesis in HCC (23,24). These findings may suggest that α-taxilin expression in HCC is associated with tumor aggressiveness represented by rapid proliferation and dedifferentiation.

In non-cancerous liver tissues, α-taxilin was weakly expressed in small numbers of hepatocytes. These hepatocytes were mainly distributed in periportal and periseptal area of liver lobule, where mitogenic activity of hepatocytes is considered to be high (25). The expression of α-taxilin in background liver might relate to the potential of hepatocyte proliferation.

At present, limited data are obtained about taxilin, and the precise function still remains unclear. Taxilin is well preserved between species, and three isoforms (α-, ß-, γ-) were reported in mammals (26). The structure of α-taxilin is characterized by a long coiled-coil domain and a leucine zipper motif. Both of them are known to be necessary for a protein-protein interaction or protein dimerization (27), and commonly found in proteins involved in important biological functions such as regulation of gene expression. The long coiled-coil domain is also a characteristic structure of proteins supporting SNARE-mediated membrane fusion (28). The SNARE proteins are localized on the restricted membrane components, and supposed to have selective function in specific intracellular trafficking steps (7). *In vitro* binding assay has shown that α-taxilin binds with some isoforms of syntaxins, specific members of SNAREs (8), which are predominantly localized on the plasma membrane and involved in post-Golgi vesicle transport. These findings lead one hypothesis that α-taxilin is involved in post-Golgi membrane traffic through its association with syntaxins localized on the plasma membrane. In addition, recent studies suggest the involvement of SNAREs and these related molecules in cell proliferation through various steps requiring membrane fusion events, such as nuclear envelope reassembly (29), cytokinesis (29-31), and organelle inheritance. α-taxilin might affect tumor growth through membrane fusion event. Furthermore, α-taxilin has been reported to have another possible binding partner unrelated to SNAREs. *In vitro* binding assay has shown that α-taxilin binds to nascent polypeptide-associated complex (NAC) (12), a ubiquitous factor of eukaryotic cells. NAC reversibly binds to newly synthesized polypeptide chains, and prevent them from improper folding or unwanted interactions with other proteins (32). This finding suggests the association of α-taxilin with translating ribosomes. Diverse functions of α-taxilin should be considered to reveal a possible mitogenic effect of α-taxilin in tumors.

New aspects have been highlighted about the function of factors associated with membrane traffic, especially SNAREs and these related proteins, in cell growth and organogenesis other than membrane fusion event. While ZW10 binds to syntaxin-18 and play a role in vesicle transport between Golgi and the endoplasmic reticulum (33), it is also known as a mitotic checkpoint protein, controlling attachment of microtubules to kinetochores of chromosomes in *Drosophila* (34). Syntaxin-2, which is localized on plasma membrane and involved in post-Golgi transport, has also been identified as an extracellular molecule playing a role in morphogenesis of epithelial organs (35) including liver (36). Overexpression of syntaxin-2 in the mouse mammary gland promotes alveolar hyperplasia and mammary adenocarcinoma (5). Syntaxin-7, which locates on endosome and mediates endosomal/lysosomal fusion events, has been reported to be associated with more aggressive phenotype of malignant melanoma (3). Syntaxin-1 has been associated with more aggressive forms of colorectal carcinomas (37). The relationship between cell proliferation and membrane traffic related proteins would be further investigated in the future.

In conclusion, the expression of the α-taxilin protein is enhanced in HCC, and related with increased proliferative activity and dedifferentiation of HCC. In addition, α-taxilin can be utilized as a marker of malignant potential of HCC.

References

1. Pang RW and Poon RT: From molecular biology to targeted therapies for hepatocellular carcinoma: the future is now. Oncology 72 (Suppl. 1): 30-44, 2007.
2. Trevisani F, Cantarini MC, Wands JR and Bernardi M: Recent advances in the natural history of hepatocellular carcinoma. Carcinogenesis 29: 1299-1305, 2008.
3. Stromberg S, Agnarsdottir M, Magnusson K, *et al*: Selective expression of Syntaxin-7 protein in benign melanocytes and malignant melanoma. J Proteome Res 8: 1639-1646, 2009.

4. Hashimoto S, Onodera Y, Hashimoto A, *et al*: Requirement for Arf6 in breast cancer invasive activities. Proc Natl Acad Sci USA 101: 6647-6652, 2004.
5. Bascom JL, Fata JE, Hirai Y, Sternlicht MD and Bissell MJ: Epimorphin overexpression in the mouse mammary gland promotes alveolar hyperplasia and mammary adenocarcinoma. Cancer Res 65: 8617-8621, 2005.
6. Rothman JE: Mechanisms of intracellular protein transport. Nature 372: 55-63, 1994.
7. Chen YA and Scheller RH: SNARE-mediated membrane fusion. Nat Rev Mol Cell Biol 2: 98-106, 2001.
8. Nogami S, Satoh S, Nakano M, *et al*: Taxilin; a novel syntaxin-binding protein that is involved in Ca^{2+}-dependent exocytosis in neuroendocrine cells. Genes Cells 8: 17-28, 2003.
9. Oba-Shinjo SM, Bengtson MH, Winnischofer SM, *et al*: Identification of novel differentially expressed genes in human astrocytomas by cDNA representational difference analysis. Brain Res Mol Brain Res 140: 25-33, 2005.
10. Sakakibara S, Nakadate K, Tanaka-Nakadate S, *et al*: Developmental and spatial expression pattern of alpha-taxilin in the rat central nervous system. J Comp Neurol 511: 65-80, 2008.
11. The Liver Cancer Study Group of Japan: The general rules for the clinical and pathological study of primary liver cancer. Kanehara & Co., Ltd., Tokyo, 2008.
12. Yoshida K, Nogami S, Satoh S, *et al*: Interaction of the taxilin family with the nascent polypeptide-associated complex that is involved in the transcriptional and translational processes. Genes Cells 10: 465-476, 2005.
13. Kitamoto M, Nakanishi T, Kira S, *et al*: The assessment of proliferating cell nuclear antigen immunohistochemical staining in small hepatocellular carcinoma and its relationship to histologic characteristics and prognosis. Cancer 72: 1859-1865, 1993.
14. Zeng WJ, Liu GY, Xu J, Zhou XD, Zhang YE and Zhang N: Pathological characteristics, PCNA labeling index and DNA index in prognostic evaluation of patients with moderately differentiated hepatocellular carcinoma. World J Gastroenterol 8: 1040-1044, 2002.
15. Yang L, Yang XC, Yang JK, *et al*: Cyclosporin A suppresses proliferation of endothelial progenitor cells: involvement of nitric oxide synthase inhibition. Intern Med 47: 1457-1464, 2008.
16. Bravo R, Frank R, Blundell PA and Macdonald-Bravo H: Cyclin/PCNA is the auxiliary protein of DNA polymerase-delta. Nature 326: 515-517, 1987.
17. Ng IO, Lai EC, Fan ST, Ng M, Chan AS and So MK: Prognostic significance of proliferating cell nuclear antigen expression in hepatocellular carcinoma. Cancer 73: 2268-2274, 1994.
18. Suehiro T, Matsumata T, Itasaka H, Yamamoto K, Kawahara N and Sugimachi K: Clinicopathologic features and prognosis of resected hepatocellular carcinomas of varied sizes with special reference to proliferating cell nuclear antigen. Cancer 76: 399-405, 1995.
19. Taniai M, Tomimatsu M, Okuda H, Saito A and Obata H: Immunohistochemical detection of proliferating cell nuclear antigen in hepatocellular carcinoma: relationship to histological grade. J Gastroenterol Hepatol 8: 420-425, 1993.
20. Yun JP, Miao J, Chen GG, *et al*: Increased expression of nucleophosmin/B23 in hepatocellular carcinoma and correlation with clinicopathological parameters. Br J Cancer 96: 477-484, 2007.
21. Kosuge T, Makuuchi M, Takayama T, Yamamoto J, Shimada K and Yamasaki S: Long-term results after resection of hepatocellular carcinoma: experience of 480 cases. Hepatogastroenterology 40: 328-332, 1993.
22. Aoki T, Inoue S, Imamura H, *et al*: EBAG9/RCAS1 expression in hepatocellular carcinoma: correlation with tumour dedifferentiation and proliferation. Eur J Cancer 39: 1552-1561, 2003.
23. Yamamoto S, Tomita Y, Nakamori S, *et al*: Elevated expression of valosin-containing protein (p97) in hepatocellular carcinoma is correlated with increased incidence of tumor recurrence. J Clin Oncol 21: 447-452, 2003.
24. Yamaguchi R, Yano H, Nakashima O, *et al*: Expression of vascular endothelial growth factor-C in human hepatocellular carcinoma. J Gastroenterol Hepatol 21: 152-160, 2006.
25. Harada K, Yasoshima M, Ozaki S, Sanzen T and Nakamura Y: PCR and *in situ* hybridization studies of telomerase subunits in human non-neoplastic livers. J Pathol 193: 210-217, 2001.
26. Nogami S, Satoh S, Tanaka-Nakadate S, *et al*: Identification and characterization of taxilin isoforms. Biochem Biophys Res Commun 319: 936-943, 2004.
27. Nishizawa M, Kataoka K, Goto N, Fujiwara KT and Kawai S: v-maf, a viral oncogene that encodes a 'leucine zipper' motif. Proc Natl Acad Sci USA 86: 7711-7715, 1989.
28. Cai H, Reinisch K and Ferro-Novick S: Coats, tethers, Rabs, and SNAREs work together to mediate the intracellular destination of a transport vesicle. Dev Cell 12: 671-682, 2007.
29. Jantsch-Plunger V and Glotzer M: Depletion of syntaxins in the early *Caenorhabditis elegans* embryo reveals a role for membrane fusion events in cytokinesis. Curr Biol 9: 738-745, 1999.
30. Low SH, Li X, Miura M, Kudo N, Quinones B and Weimbs T: Syntaxin 2 and endobrevin are required for the terminal step of cytokinesis in mammalian cells. Dev Cell 4: 753-759, 2003.
31. Prekeris R and Gould GW: Breaking up is hard to do - membrane traffic in cytokinesis. J Cell Sci 121: 1569-1576, 2008.
32. Rospert S, Dubaquie Y and Gautschi M: Nascent-polypeptide-associated complex. Cell Mol Life Sci 59: 1632-1639, 2002.
33. Hirose H, Arasaki K, Dohmae N, *et al*: Implication of ZW10 in membrane trafficking between the endoplasmic reticulum and Golgi. EMBO J 23: 1267-1278, 2004.
34. Karess R: Rod-Zw10-Zwilch: a key player in the spindle checkpoint. Trends Cell Biol 15: 386-392, 2005.
35. Chen CS, Nelson CM, Khauv D, *et al*: Homology with vesicle fusion mediator syntaxin-1a predicts determinants of epimorphin/syntaxin-2 function in mammary epithelial morphogenesis. J Biol Chem 284: 6877-6884, 2009.
36. Miura K, Yoshino R, Hirai Y, *et al*: Epimorphin, a morphogenic protein, induces proteases in rodent hepatocytes through NF-kappaB. J Hepatol 47: 834-843, 2007.
37. Grabowski P, Schonfelder J, Ahnert-Hilger G, *et al*: Expression of neuroendocrine markers: a signature of human undifferentiated carcinoma of the colon and rectum. Virchows Arch 441: 256-263, 2002.

Journal of Medical Virology 82:776–782 (2010)

Hepatitis C Virus Core Protein Compromises Iron-Induced Activation of Antioxidants in Mice and HepG2 Cells

Kyoji Moriya, Hideyuki Miyoshi, Seiko Shinzawa, Takeya Tsutsumi, Hajime Fujie, Koji Goto, Yoshizumi Shintani, Hiroshi Yotsuyanagi, and Kazuhiko Koike*

Department of Internal Medicine, Graduate School of Medicine, University of Tokyo, Tokyo, Japan

One of the characteristics of hepatitis C virus (HCV) infection is the unusual augmentation of oxidative stress, which is exacerbated by iron accumulation in the liver, as observed frequently in hepatitis C patients. Using a transgenic mouse model, the core protein of HCV was shown previously to induce the overproduction of reactive oxygen species (ROS) in the liver. In the present study, the impact of iron overloading on the oxidant/antioxidant system was examined using this mouse model and cultured cells. Iron overloading caused the induction of ROS as well as antioxidants. However, the augmentation of some antioxidants, including heme oxygenase-1 and NADH dehydrogenase, quinone 1, was compromised by the presence of the core protein. The attenuation of iron-induced augmentation of heme oxygenase-1 was also confirmed in HepG2 cells expressing the core protein. This attenuation was not dependent on the Nrf2 transcription factor. Thus, HCV infection not only induces oxidative stress but also hampers the iron-induced antioxidant activation in the liver, thereby exacerbating oxidative stress that would facilitate hepatocarcinogenesis. ***J. Med. Virol. 82:776–782, 2010.*** © 2010 Wiley-Liss, Inc.

KEY WORDS: oxidative stress; transgenic mouse; hepatocellular carcinoma; antioxidant; heme oxygenase-1

INTRODUCTION

Hepatitis C virus (HCV) is a major cause of liver disease. Persistent HCV infection leads to the development of chronic hepatitis, cirrhosis, and, eventually, hepatocellular carcinoma (HCC), thereby being a serious problem both in medical and socio-economical aspects [Saito et al., 1990]. Despite overwhelming evidence from epidemiological studies, the precise mechanism of hepatocarcinogenesis in HCV infection is still not fully understood. Recently, it has been shown that the core protein of HCV induces HCC in transgenic mice [Moriya et al., 1998; Naas et al., 2005; Machida et al., 2006]. Augmentation of oxidative stress is implicated in the pathogenesis of liver disease in HCV infection as shown by a number of clinical and basic studies [Farinati et al., 1995; Moriya et al., 2001; Choi and Ou, 2006]. Reactive oxygen species (ROS) are endogenous oxygen-containing molecules formed as normal products during aerobic metabolism. ROS can induce genetic mutations as well as chromosomal alterations and thus contribute to cancer development in multistep carcinogenesis [Fujita et al., 2008]. Recent studies have shown that oxidative stress is more augmented in hepatitis C than in other types of hepatitis such as hepatitis B [Farinati et al., 1995; Chapoutot et al., 2000]. On the other hand, in chronic hepatitis C, HCC and fibrosis are closely associated with the amount of iron in the liver. Iron depletion both in the form of dietary iron restriction or phlebotomy improved hepatic inflammation and lowered serum aminotransferase levels in hepatitis C patients. Phlebotomy decreases the hepatic content of 8-OH deoxyguanosine, a marker of DNA damage, improved inflammation and fibrosis

Abbreviations: HCV, hepatitis C virus; HCC, hepatocellular carcinoma; ROS, reactive oxygen species; HO-1, heme oxygenase-1; thiobarbituric acid reactive substances (TBARS); GST, glutathione-*S*-transferase; SOD, superoxide dismutase; GPx, glutathione peroxidase; NQO1, NAD(P)H dehydrogenase, quinone 1; AP-1, activator protein-1; NF-κB, nuclear factor-kappa B; Bach1, BTB and CNC homology 1.

Grant sponsor: Ministry of Education, Culture, Science, Sports and Technology of Japan (Grant-in-Aid for Scientific Research on Priority Area, partly supported); Grant sponsor: Ministry of Health, Labor and Welfare (Health Sciences Research Grants, Research on Hepatitis).

*Correspondence to: Kazuhiko Koike, MD, Department of Gastroenterology, Graduate School of Medicine, University of Tokyo, 7-3-1 Hongo, Bunkyo-ku, Tokyo 113-8655, Japan.
E-mail: kkoike-tky@umin.ac.jp

Accepted 11 August 2009

DOI 10.1002/jmv.21661

Published online in Wiley InterScience (www.interscience.wiley.com)

scores, and prevented HCC development [Kato et al., 2001].

Thus, a major role in the pathogenesis of HCV-associated liver disease has been attributed to oxidative stress augmentation, in association with iron accumulation, but no underlying mechanism is understood well yet. Hence, it is an important issue to understand the mechanism of oxidative stress augmentation, which may allow us to develop new tools of therapies for chronic hepatitis C. Iron accumulation and oxidant/antioxidant status were assessed with or without iron overloading in the liver of a transgenic mouse model of HCC in HCV infection. The expression levels of genes associated with the antioxidant system were also determined.

MATERIALS AND METHODS

Transgenic Mice and Cultured Cells

The production of HCV core gene transgenic mice has been described previously [Moriya et al., 1998]. Briefly, the core gene of genotype 1b HCV was introduced into C57BL/6 mouse embryos (Clea Japan, Tokyo, Japan). Mice were cared for according to institutional guidelines approved by the institutional review board of the animal care committee, fed an ordinary chow diet (Oriental Yeast Co., Ltd, Tokyo, Japan), and maintained in a specific pathogen-free state. At least five mice were used for each experiment and the data were subjected to statistical analysis.

Determination of Iron in the Liver

Determination of Fe in the liver was performed by Shimadzu Techno-Research, K.K. (Kyoto, Japan) using Inductively Coupled Plasma apparatus, ICP8100 (Shimadzu Corp.). Briefly, samples were resolved by microwave (Microwave Resolution System ETHOS-TC, Milestone General, Inc., Tokyo, Japan) after the addition of nitric acid, and the volume was adjusted by the addition of H_2O. This solution was then subjected to the quantification of iron using ICP8100 (http://www.shimadzu.com/products/lab/ms/glossary/oh80jt00000008w4.html).

Iron Loading Experiments

For the short-term iron loading experiment, three doses of $FeSO_4$ solution (100 mg/kg BW, suspended in dH_2O) or vehicle only were administered to the core gene transgenic or control mice i.p., with intervals of 24 hr at the age of 6 months [Zhu and Miller, 2007]. For the long-term iron loading experiment, 50 mg/kg BW of $FeSO_4$ was administered to the core gene transgenic mice i.p., once a week for 3 months from the age of 3 months. HepG2 cell lines expressing the HCV core protein under the control of the CAG promoter (Hep39J, Hep396, and Hep397) or a control HepG2 line (Hepswx) carrying the empty vector were described previously [Ruggieri et al., 2004]. For the iron loading experiments, hemin solution (10 mM in DMSO) was added to the culture medium at the final concentration of 5 μM, and the cells were incubated for 5 or 72 hr.

Evaluation of Oxidant and Antioxidant Systems

Lipid peroxidation in the liver was estimated spectrophotometrically using thiobarbituric acid reactive substances (TBARS) and is expressed in terms of malondialdehyde formed per milligram protein. In the cell culture experiment, the cells were examined for ROS production using chloromethyl 2′,7′-dichlorodihydrofluorescein diacetate (Molecular Probes, Inc., Eugene, OR). For the evaluation of DNA damage in cells, apurinic/apyrimidinic (AP) sites were determined using a DNA Damage Quantification Kit (Dojindo Molecular Technologies, Inc., Tokyo, Japan).

Real-Time PCR and Western Blotting

RNA was prepared from mouse liver tissues using TRIzol LS (Invitrogen, Carlsbad, CA). The first-strand cDNAs were synthesized with a first-strand cDNA synthesis kit (Amersham Pharmacia Biotech, Franklin Lakes, NJ). The fluorescence signal was measured using ABI Prism 7000 (Applied Biosystems, Tokyo, Japan). Primers and probes for hepcidin (Unigene ID: Mm. 439939), catalase (Mm. 4215), glutathione-*S*-transferase (GST) (Mm. 1090), superoxide dismutase (SOD)1 (Mm. 01344233), glutathione peroxidase (GPx)1 (Mm. 1090), heme oxygenase (HO)-1 (Mm. 00516004), NAD(P)H dehydrogenase, quinone (NQO) 1 (Mm. 500821), activator protein (AP)-1 (Mm. 275071), nuclear factor-kappa B (NF-κB)1 (Mm. 256765), BTB and CNC homology (Bach)1 (Mm. 26147), and hypoxanthine phosphoribosyltransferase (Mm. 299381) were purchased as assays-on-demand (Applied Biosystems). Each cDNA prepared was used in triplicate for the real-time PCR procedures for each gene tested.

Western blotting was performed with an anti-HO-1 antibody (Stressgen Biotechnologies, Corp., Victoria, BC, Canada) or anti-Nrf2 antibody (Santa Cruz Biotechnology, Santa Cruz, CA), and Super Signal Femto (Pierce, Rockford, IL).

Statistical Analysis

Data are presented as the mean ± SE. The significance of the difference in means was determined by Mann–Whitney's *U*-test. $P < 0.05$ was considered significant.

RESULTS

Iron Accumulation in Ordinarily Fed Core Gene Transgenic Mice

The core gene transgenic mice develop HCC after an incubation period of approximately 16 months, in the absence of inflammation [Moriya et al., 1998]. During the incubation period, there is augmentation of oxidative stress with a concomitant activation of antioxidants and development of DNA damage in the liver [Farinati

et al., 1995]. For mice fed with normal chow, the concentration of total iron in the liver was higher in the core gene transgenic mice than in the control mice, and the difference became significant after the age of 12 months (Fig. 1A). The level of hepcidin mRNA, the product of which maintains iron homeostasis by a direct inhibition of ferroportin [Muckenthaler, 2008], was significantly higher in the core gene transgenic mice than in the control mice at the age of 3 and 15 months (Fig. 1B).

Iron Overloading to Core Gene Transgenic Mice

When the mice were overloaded with iron, the intrahepatic levels of iron markedly increased. In the short-term iron loading (for three consecutive days at the age of 6 months), the iron concentration in the iron-treated mice was more than twofold higher than that in the vehicle-treated ones in both the core gene transgenic and control mice, but there was no difference between the core gene transgenic and control mice. In the long-term iron loading (for 3 months from the age of 3 months), the iron concentration became significantly higher in the core gene transgenic mice than in the control mice (Fig. 1C). The hepcidin mRNA level was proportionally higher in the long-term iron-loaded mice than in the vehicle-treated mice and was significantly higher in the core gene transgenic than in the control mice ($P < 0.05$, Fig. 1D), suggesting that the positive feedback from iron to hepcidin is instrumental.

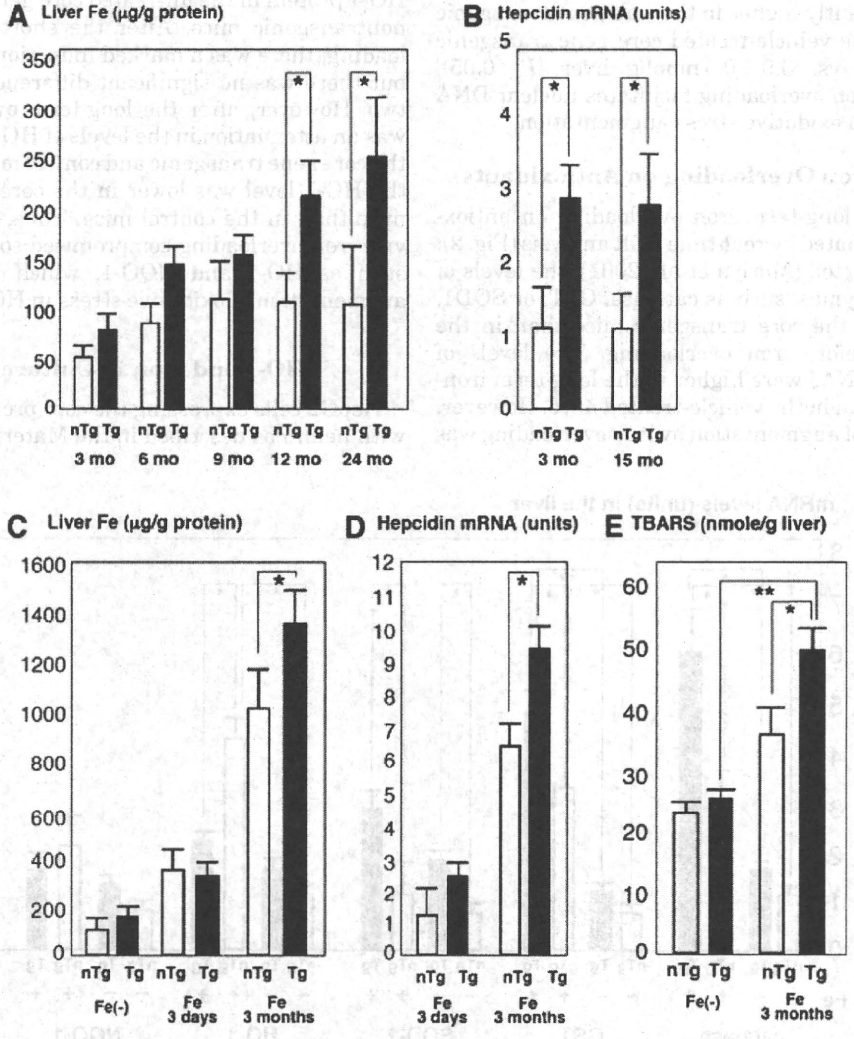

Fig. 1. **A**: Amounts of iron accumulated in the liver of mice fed with normal chow. **B**: Hepcidin mRNA level in the liver of mice fed with normal chow at 3 and 15 months. **C**: Amounts of iron in the liver of mice subjected to iron overloading for 0, 3 days, or 3 months. **D**: Hepcidin mRNA level in the liver of mice subjected to iron overloading for 0, 3 days, or 3 months. **E**: Oxidative stress in the liver of mice subjected to iron overloading for 0 or 3 months. The data represent means ± SE, n = 5 in each group. $^{*}P < 0.05$, $^{**}P < 0.01$. nTg, nontransgenic control mice; Tg, transgenic mice; TBARS, thiobarbituric acid reactive substances.

Oxidative Stress and Iron Overloading in Mice

As described previously, ROS production in the liver of the core gene transgenic mice is already augmented at the young age, but the lipid peroxidation level is not higher than that in the control mice due to the concomitant activation of antioxidant system [Moriya et al., 2001]. This was also the case in the current experiment: there was no significant difference in the ROS level at the age of 6 months between the core gene transgenic and control mice that were treated with the vehicle, as determined by TBARS (Fig. 1E). However, after the long-term iron treatment, ROS levels in the liver of the core gene transgenic mice became significantly higher than that in the control mice (Fig. 1E, $P < 0.05$). After the long-term iron treatment, the AP site index, a marker for nuclear DNA damage, became significantly higher in the core gene transgenic mice than in the vehicle-treated core gene transgenic mice (5.2 ± 0.6 vs. 3.9 ± 0.3 nmol/g liver, $P < 0.05$), showing that iron overloading facilitates nuclear DNA damage through oxidative stress augmentation.

Impact of Iron Overloading on Antioxidants

The effect of long-term iron overloading on antioxidants was evaluated by real-time PCR analysis (Fig. 2). As already reported [Moriya et al., 2001], the levels of antioxidant enzymes, such as catalase, GST, or SOD1, were higher in the core transgenic mice than in the control mice before iron overloading. The levels of antioxidant mRNAs were higher in the long-term iron-treated mice than in the vehicle-treated mice. However, the magnitude of augmentation by iron overloading was different among the antioxidant genes. While catalase and GST genes were significantly more enhanced in the core gene transgenic mice than in the control mice by iron overloading ($P < 0.05$), there was less augmentation in the expressions of HO-1 and NQO-1 genes in the core gene transgenic mice than in the control mice. The level of HO-1 mRNA in the long-term-treated mice was significantly higher in the control mice than in the core gene transgenic mice ($P < 0.05$, respectively), in contrast to that of catalase, GST, or SOD1 gene. The level of NQO-1 mRNA in the liver was lower in the core gene transgenic than in the control mice, although the difference was not statistically significant.

To confirm this observation, the protein level of HO-1 was determined by Western blotting. As shown in Figure 3A, there was only a marginal expression of HO-1 protein in the untreated core gene transgenic and nontransgenic mice. After the short-term iron overloading, there was a marked induction of HO-1 protein but there was no significant difference between these two. However, after the long-term overloading, there was an attenuation in the levels of HO-1 protein in both the core gene transgenic and control mice; in particular, the HO-1 level was lower in the core gene transgenic mice than in the control mice. Thus, the long-term in vivo iron overloading compromised some antioxidants, such as HO-1 and NQO-1, which may lead to an augmentation of oxidative stress in HCV infection.

HO-1 and Iron in Cultured Cells

HepG2 cells expressing the core protein were treated with hemin as described in the Materials and Methods

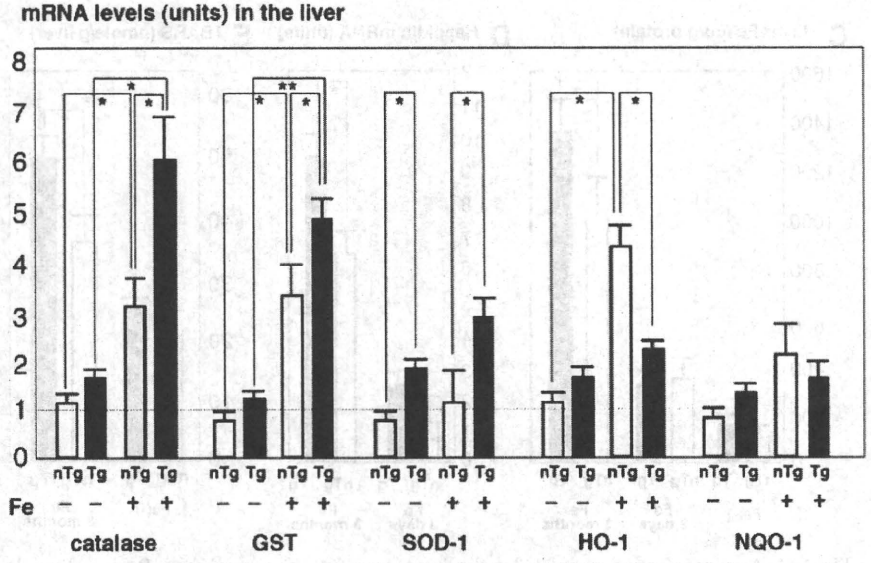

Fig. 2. Levels of antioxidant mRNA in the liver of mice subjected to iron overloading. Levels of mRNA were determined in nontransgenic control mice (open bars) or in transgenic mice (closed bars) with 3-month administration of iron (Fe+) or without it (Fe−). Mice were sacrificed at 6 months and liver tissues were subjected to determination. The data represent means ± SE, n = 5 in each group. $^*P < 0.05$, $^{**}P < 0.01$. nTg, nontransgenic control mice; Tg, transgenic mice; GST, glutathione-*S*-transferase: SOD1, superoxide dismutase 1; HO-1, heme oxygenase 1; NQO-1, NAD(P)H dehydrogenase, quinone 1.

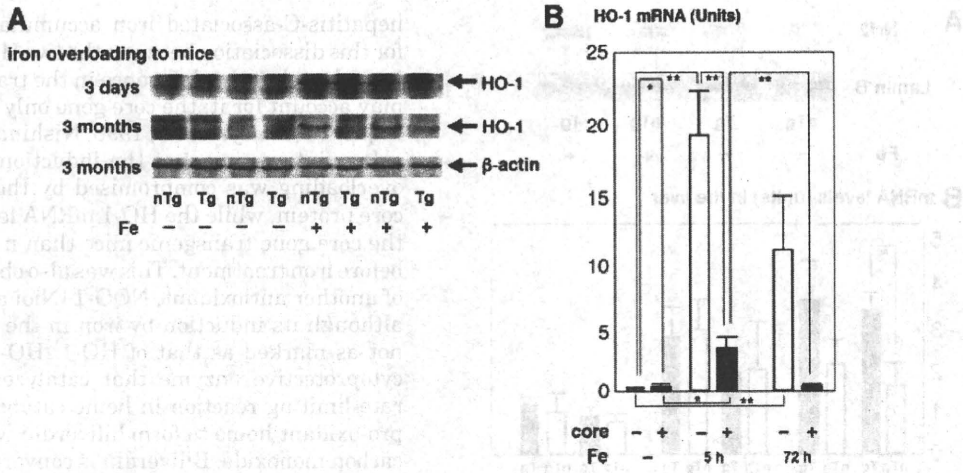

Fig. 3. **A**: Levels of HO-1 protein determined by Western blotting in the liver of mice subjected to iron overloading for 0, 3 days, or 3 months. **B**: Levels of HO-1 mRNA in core-protein-expressing or nonexpressing HepG2 cells subjected to iron loading for 0, 5, or 72 hr. nTg, non-transgenic control mice; Tg, transgenic mice; HO, heme oxygenase.

Section. Before the treatment, the HO-1 mRNA level was significantly higher in the core-expressing cells than in the control HepG2 cells (Fig. 3B, 1.00 ± 0.33 vs. 0.19 ± 0.10 arbitrary units, $P < 0.05$). After the short-term iron treatment (for 5 hr), the HO-1 mRNA levels increased in both cell lines but it was significantly higher in the control cells than in the core-expressing cells (Fig. 3B, $P < 0.01$). After the long-term iron treatment (72 hr), there was a decrease in the HO-1 mRNA levels in both cell lines compared with those after the short-term iron treatment, but the magnitude of decrease was marked in the core-expressing cells ($P < 0.05$, 5 hr core (+) vs. 72 hr core (+)). Thus, the core protein compromised the iron-induced enhancement of HO-1, and such an effect of the core is more prominent in the long-term iron overloading than in the short-term one. Thus, both in mice and cultured cells, the iron-induced induction of HO-1 was compromised by the presence of the core protein. Similar to the iron-overloading experiment in mice, iron treatment induced ROS production in cultured cells to a greater extent in the core-expressing cells than in control cells (data not shown).

Absence of Nrf2 Involvement in HO-1 Impairment by the Core Protein

To explore the mechanism underlying the differential responses to iron overloading in antioxidant gene expressions, the intracellular distribution of a transcription factor, Nrf2, which regulates the expression of HO-1 [Srisook et al., 2005; Farombi and Surh, 2006] was examined. For this analysis, the liver tissues from the core gene transgenic and control mice, either iron-overloaded or not, were subjected to subcellular fractionation, followed by detection by Western blotting. However, there was no decrease or rather an increase in the Nfr2 level localized in the nuclear fraction after the iron-overloading treatment in the core transgenic mouse liver (Fig. 4A), indicating that the attenuation of HO-1 expression is not dependent on Nrf2. Finally, no interaction was observed between the core protein and the Nrf2 protein as determined by coimmunoprecipitation using cultured cells (data not shown). Because transcription factors, other than Nrf2, such as AP-1 and NF-κB, may be responsible for the HO-1 gene expression [Ferrándiz and Devesa, 2008], and Bach1, an HO-1 repressor [Shan et al., 2004], may be responsible for the attenuation of HO-1 expression, changes in expression levels of these factors were determined by the real-time PCR. AP-1 was activated by the core protein while NF-κB was not in the liver of transgenic mice [Tsutsumi et al., 2002]. With the administration of iron, mRNA levels of AP-1 and NF-κB1 were increased slightly both in core gene transgenic and control mice (Fig. 4B), thereby not explaining the attenuation of iron-induced HO-1 induction by the core protein. Bach1 expression level was not changed significantly by iron administration in the core gene transgenic mice (Fig. 4B), negating the possibility that this repressor acts to inhibit the induction of HO-1 gene expression by iron.

DISCUSSION

Chronic hepatitis C is characterized by its prominent augmentation of oxidative stress [Choi and Ou, 2006; Fujita et al., 2008; Moriya et al., 2001]. Iron accumulation in the liver has been shown to aggravate the oxidative stress as shown by the increase in the amount of DNA adducts in the liver [Chapoutot et al., 2000; Moriya et al., 2001; Choi and Ou, 2006; Fujita et al., 2008]. In this study, iron was accumulated in the liver of the HCV core gene transgenic mice, which is destined to develop HCC after a certain period with increased